

Installation and Thermal Feedback from a Multi-wavelength Pyrometer in Electron Beam Melting

Jonathan Minjares¹, Jorge Mireles¹, Sara M. Gaytan¹, David Espalin¹, William T. Carter², and Ryan B. Wicker¹

¹W.M. Keck Center for 3D innovation, The University of Texas at El Paso, El Paso, Texas, 79968

²GE Global Research, Niskayuna, NY, 12309

Abstract

The purpose of this paper is to outline and discuss the installation and use of a multi-wavelength pyrometer for process temperature monitoring in Electron Beam Melting (EBM). A multi-wavelength pyrometer was externally mounted atop an EBM system to observe and record surface temperatures during the fabrication process. The multi-wavelength pyrometer is a non-contact device capable of measuring the temperature of an object without the need of knowing the object's emissivity. Temperature data from the EBM system thermocouple and the multi-wavelength pyrometer were compared, and it was determined that the pyrometer measurements were reasonable. During fabrication, the multi-wavelength pyrometer allowed the characterization of the EBM process that consisted of various steps during fabrication (e.g. heating of the build platform, powder deposition, and melting). Measurement of surface temperatures during fabrication can be useful for parameter development of novel materials, prediction of resulting microstructural architectures, and ultimately as feedback used in a closed-loop control system, allowing full spatial and temporal control of melting and microstructure.

1. Introduction

Additive manufacturing (AM) is a process that consists of adding layers of a material to create a solid 3D object starting from a computer-aided-design (CAD) (Sclater and Chironis, 2006). The Electron Beam Melting (EBM) process is an AM technology to develop end-use metal components in industries, such as aerospace, biomedical, electrical, and automotive (Gibson *et al.*, 2010). Material development on this system is of significant interest, because it can inherently produce dense parts with reduced residual stresses compared to similar powder fusion processes like selective laser melting. However, material development is not trivial and can benefit from added process feedback. In commercial EBM systems, temperature feedback consists of a single thermocouple that measures the temperature below the build platform. However, since the EBM is a layer-by-layer process, the temperature readings are not representative of the layer being fabricated and do not show the surface temperatures to perceive any effect on the quality of the part (e.g. microstructure variations from different thermal conditions). When developing processing parameters or attempting to control microstructure, it is important to know the surface temperature during fabrication. With the added capability of knowing the temperature for each process step, the operator can modify system parameters to obtain a desired surface temperature.

Methods to understand the temperature of the forming layer have been attempted to analyze the thermal environment of the EBM system while fabricating. In a study conducted by Price *et al.* (2013), an infrared (IR) camera was used in an EBM system to analyze the melt pool sizes and temperature distributions around the melting area at various configurations, finding peak temperatures during the melting step, molten pool emissivity, and small differences in temperature profiles as the build increases in height. Additionally, Rodriguez (2013) recorded thermal images to obtain the post-melting temperature of the forming by utilizing an IR camera with a specified emissivity value for EBM while processing Ti-6Al-4V. Utilization of an IR camera in EBM has allowed analysis of thermal images to detect defects such as porosity and the development of automated control for microstructure and process control (Mireles, 2013). The studies performed by Rodriguez and Mireles utilized a shutter mechanism to avoid metallization of the view window, due to elements condensing and evaporating from the melt pool. Oak Ridge National Laboratory developed a shutterless mechanism to obtain real-time thermal images using a moving Mylar film canister to improve the reliability of the EBM process (Dinwiddie, *et al.*, 2013).

The work from these authors focuses on infrared emissions as a source of thermal information; however, varying factors such as radiant temperature and emissivity can affect the thermal measurement. A multi-wavelength pyrometer was used in this research, which is a device that calculates the surface temperature of a target object without the need of knowing emissivity. A multi-wavelength pyrometer was externally mounted atop an EBM system to monitor the surface temperature during the fabrication process. Temperature data from the pyrometer was compared to that of a thermocouple. The pyrometer allowed the characterization of the EBM process, such as powder deposition, preheating, melting, and cooling during layer-by-layer fabrication. This information can be useful when developing and improving parameters for a new material or to improve its mechanical properties by further controlling the thermal environment during fabrication. Furthermore, the temperatures profiles obtained can give an approximation of the solidification phenomena that occurs during each layer, which may be useful to achieve full spatial and temporal control of microstructure.

2. Methodology

2.1 EBM system

EBM consists of several steps to fabricate a part (powder deposition, preheating, and melting). First, a layer (~0.07mm in thickness) of powder is deposited into the build platform by a powder deposition mechanism. The electron beam preheats the powder to about 50% of the melting temperature of the alloy (~760°C for Ti-6Al-4V), which is used to sinter the powder around the part to hold the part during the fabrication process (Cormier *et al.*, 2004). Furthermore, preheating helps decrease the thermal gradient between layers and throughout the overall part, thus, reducing thermal stresses (Cormier *et al.*, 2004). After the preheat cycle, the electron beam melts the metal powder following the 2D cross section from a sliced computer-aided design (CAD) model. The start plate is lowered by the thickness of one layer and the steps of powder deposition, preheating, and melting are repeated until fabrication is complete (Cormier *et al.*, 2004).

2.2 Multi-wavelength pyrometer

The pyrometer specified in this study has been previously used to measure processing temperature of metals in hostile thermal environments where the emissivity is changing or unknown such

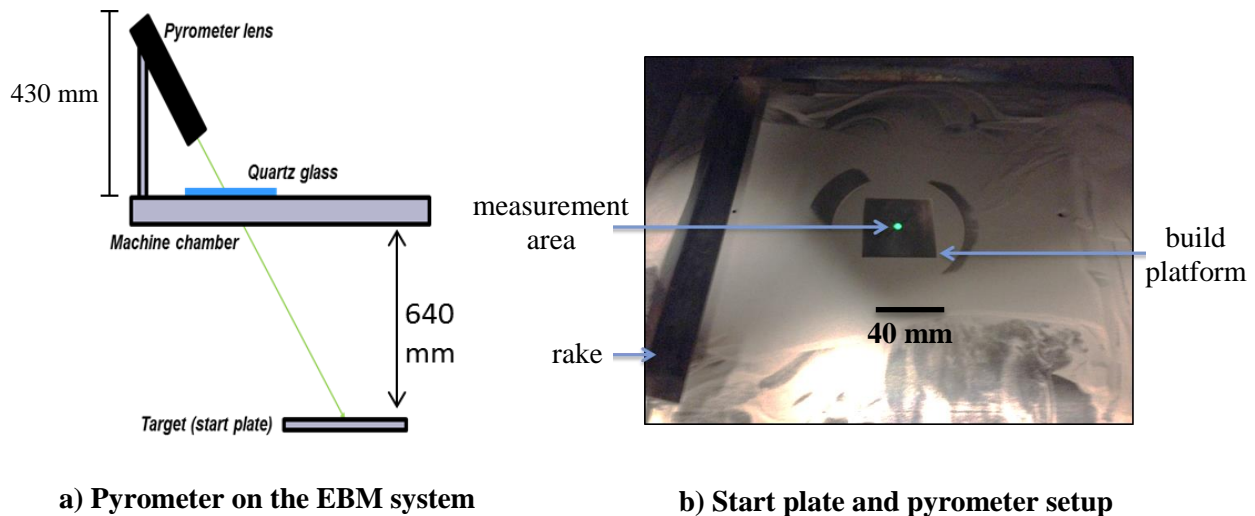


Figure 1 a) Pyrometer setup schematic, b) laser spot specifying area where pyrometer obtained data

as investment casting. The multi-wavelength pyrometer has been able to identify and discard radiation affected by the process's gas emissions or absorptions (Felice, 2006). The pyrometer is a non-contact device capable of measuring the temperature of an object without the need of knowing emissivity, or the object's surface ability to emit radiant energy (Felice, 2002). To automatically determine an emissivity, the instrument measures the target object's wavelengths to calculate a temperature whose radiance curve is compared to an ideal Planck curve. If the curve matches, the target is said to be an ideal blackbody (emissivity=1), otherwise the radiance corresponds to a non-blackbody and emissivity is automatically calculated to match a Planck curve. In this research, the multi-wavelength pyrometer was externally mounted atop an EBM system pointing to the build platform within the vacuum chamber through a quartz window (which allowed ~99% transmission for detected wavelengths) (Figure 1a). For all experiments presented in this paper, the pyrometer was pointed to the middle of the build platform and all recorded temperature data corresponded to the part fabricated at that location. Figure 1b illustrates the position of the pyrometer where the spot within the build platform is the measurement area (~2mm diameter) of the pyrometer. The multi-wavelength pyrometer functions by using a fiber optic cable that directs light to the object whose temperature is being measured and detects the wavelengths emitted by using a spectrophotometer that separates the detected wavelengths. By employing an electrical transmission line, the information is sent to the device's analog-to-digital conversion system, which computes and reports

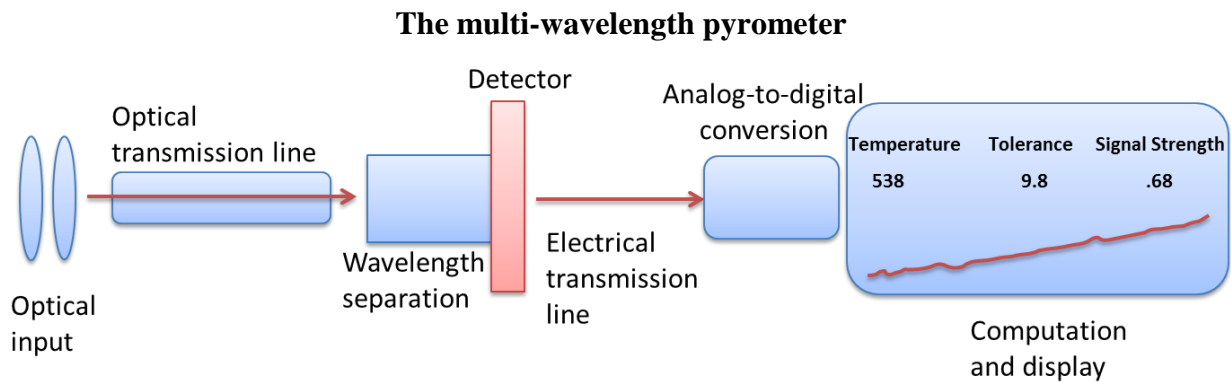
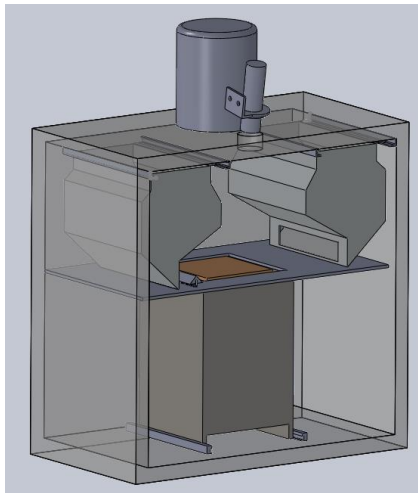


Figure 2. Schematic of the multi-wavelength pyrometer

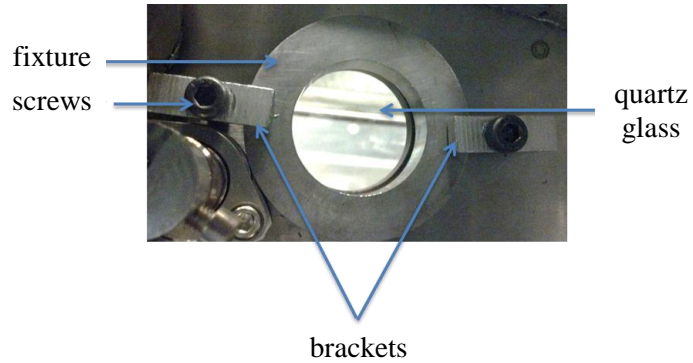
temperature, tolerance, and signal strength that is displayed in a desktop computer. Figure 2 illustrates the schematic of the multi-wavelength pyrometer used in this study. The multi-wavelength pyrometer is able to measure temperatures in the range of 300°C to 2,000°C. While measuring, the pyrometer displays and records 1) temperature of the target object (in °C), 2) tolerance of the measured temperature (standard deviation), and 3) signal strength (an emissivity value at a certain wavelength) (Felice, 2003).

2.3 Installation of pyrometer on EBM system

In its commercial state, the EBM system includes a standard video camera to observe part fabrication that was removed to install the multi-wavelength pyrometer. Fixtures and brackets were designed and fabricated to maintain a good seal on the top of the chamber and ensure the system was able to obtain appropriate vacuum levels for fabrication (~10⁻⁴ torr). The fixture consisted of a stainless steel ring that fit the outside contour of the quartz glass, and two aluminum brackets were used to press the fixture onto the glass using screws. A quartz glass (~70mm in diameter by ~10mm in thickness) was



a) Pyrometer pointing inside the EBM system



b) Fixture and brackets installed on the EBM System

Figure 3 Pyrometer and fixture

utilized to obtain optimum transmission of light waves. Figure 3a illustrates the pyrometer looking through the inside of the system and Figure 3b shows the fixture and the bracket installed on the system.

2.4 Radiation shielding

During the fabrication process, X-rays are emitted by electrons generated from the electron beam. The vacuum chamber, the lead-coated glass windows, and the heat shields are specifically designed to enclose the emitted X-rays, allowing the external emissions to remain within approved levels. Installation of a radiation shield was crucial to prevent radiation exposure of harmful X-rays to the EBM user since the original bracket from the camera was removed, and the lead-coated glass was replaced with a quartz glass. The shield design consisted of a thin plate with a curvature around the quartz glass fixture and a hollow cylinder on top of the fixture to prevent radiation exposure and hold the pyrometer in place. Stainless steel was used for both the thin plate and the hollow cylinder and covered with lead foil. A cap was designed to fill any space between the hollow cylinder and the pyrometer. The cap was fabricated by AM using a U-print system and also covered with lead foil post-fabrication. Figure 4a illustrates the CAD model for the radiation shield and Figure 4b describes the radiation shield installed on the EBM system. Radiation levels were measured while the machine was in operation post-installation using a Geiger counter to ensure no harmful radiation was emitted from the system.

2.5 Quartz glass metallization

The pyrometer pointed to the inside of the EBM system through a quartz glass window. When the electron beam melts the metal powder, elements with low melting temperatures (e.g. aluminum) vaporize, causing metallization on the quartz glass since the quartz glass is non-conductive and thus more susceptible to metallization. After a certain period of time, metallization will decrease the accuracy of the pyrometer to the extent where the pyrometer stops displaying data. The time of the quartz glass metallizing depends on the size of the layer being formed. Thus, the larger the cross section being melted, the greater the vaporization, which causes the quartz glass to metallize faster. For this reason, a process to remove metallization was implemented. The procedure consisted of 1) cleaning the quartz glass with isopropyl alcohol, 2) the quartz glass was polished in a standard 8 inch (203mm) rotating wheel using a

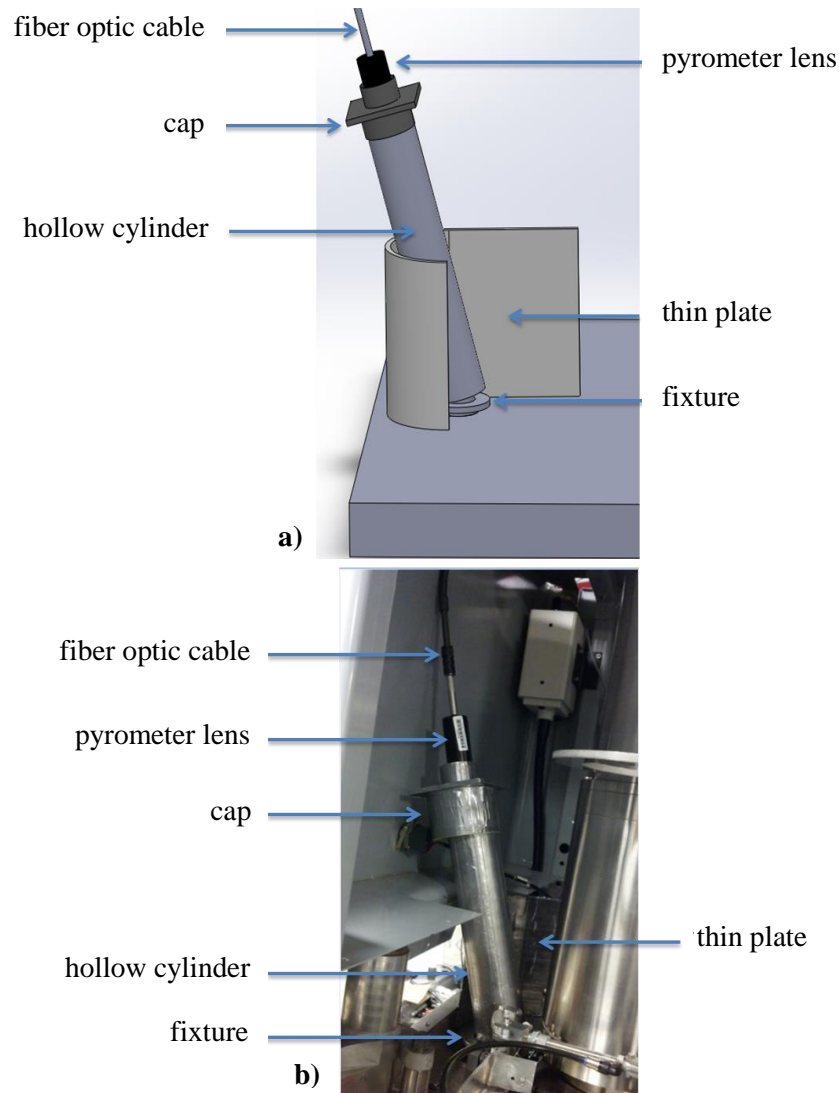


Figure 4 Radiation shield a) Radiation shield CAD model, b) Radiation shield installed in the EB system

soft cloth and alumina of $1\mu\text{m}$, 3) the glass was rotated 90° to have an even surface, and 4) polished until metallization was removed.

2.6 Description of custom experiments

An experiment was performed to compare the effect on the pyrometer's measurements between the use of a new and a polished quartz glass. That is, the polishing process was suspected to alter the reflection and transmission of light to the instrument. The experiment consisted of pointing the pyrometer to a digital hot plate set to its maximum temperature of $\sim 530^\circ\text{C}$. When the pyrometer temperature measurement was stable, a new quartz glass was placed between the pyrometer and the hot plate. Then, the new quartz glass was removed and replaced with a polished quartz glass.

Also of interest was the acquisition of reasonable data obtained from the pyrometer. Thus, an experiment was performed that consisted of drilling a hole in the middle of a standard build platform (150 by 150 by 10mm Stainless Steel plate) to expose a thermocouple to the surface and obtain measurements subsequently with the pyrometer. The multi-wavelength pyrometer was pointed to the start plate with the

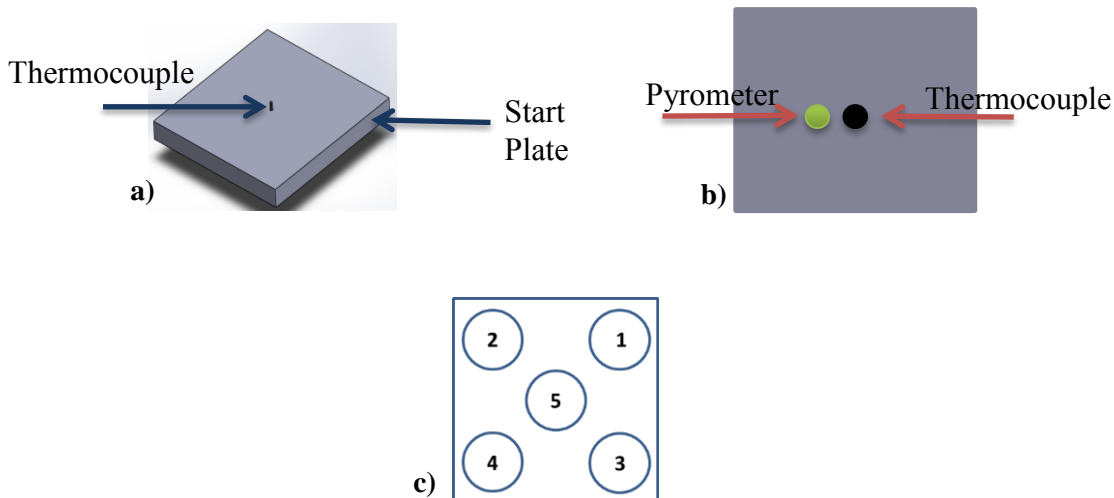


Figure 5 Experimental setup for a) comparison of temperature data between the pyrometer and the thermocouple, b) Top view showing the location of the pyrometer's spot size and the thermocouple, and c) part arrangement to characterize the EBM process

spot size next to the thermocouple to compare temperature readings. The start plate was heated by the electron beam, the process was stopped, and the plate was allowed to cool down to room temperature. Figure 5a shows the commercially installed thermocouple in the center of the start plate and Figure 5b describes the spot size of the pyrometer and the thermocouple. The temperature data were graphed utilizing MATLAB to compare the temperature measurements between the multi-wavelength pyrometer and the system's thermocouple.

Finally, characterization of the EBM process was performed. An experiment was conducted using a method (shown in Figure 5c) consisting of five cylinders each 10mm in diameter and 10mm in height located within a small start plate (40 by 40 by 10mm). During the experiment, the pyrometer was pointed to the center part (labeled 5) and temperature data was taken throughout every step of fabrication.

3. Results and Discussions

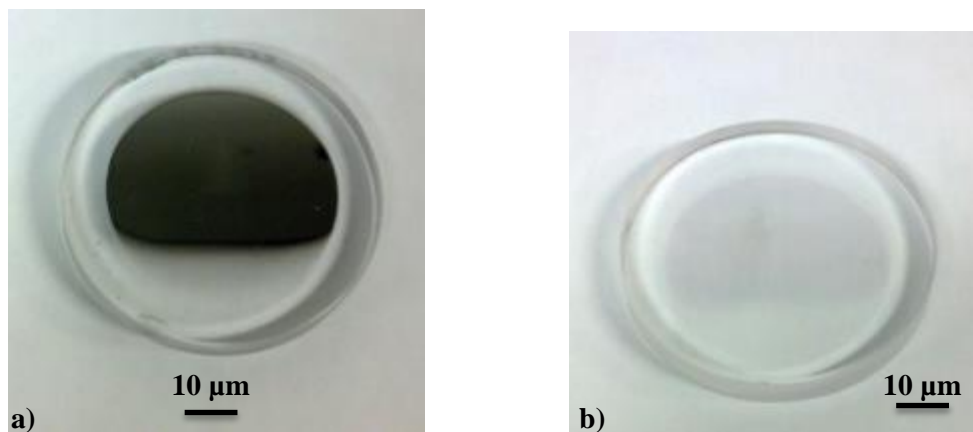


Figure 6. Quartz glass a) Metallized quartz glass, b) Polished quartz glass

The installed radiation shield was found to be effective in preventing leakage radiation. It was found that the Geiger counter did not detect harmful levels of radiation emitted by the EBM during operation. Furthermore, the comparison between a new and a polished quartz glass revealed the pyrometer displayed a $\sim 1^\circ\text{C}$ temperature change that was considered negligible. Figure 6 illustrates a metallized and a quartz glass after polishing. Future work may be performed to avoid metallization of the quartz glass, such as implementing a revolving quartz film. The above results verified that the installation and setup procedures of the pyrometer in EBM were safe and effective for data acquisition.

Results to compare the temperature data from the instrument (experiment in Figure 5 (a & b)) are shown in Figure 7 where the red plot in the figure is the thermocouple data, and the blue plot is data obtained from the multi-wavelength pyrometer. The initial peak on the blue plot is due to the pyrometer calibration (i.e., the pyrometer was filtering particular wavelengths that did not correspond to the detected spectra). Initially, the temperature data are in close agreement, then, the thermocouple data intersects with the pyrometer data showing a higher temperature. This discrepancy may be due to the beam scanning directly onto the thermocouple. After the process was stopped, both temperatures were approximately equal. Nonetheless, the average percent difference between the thermocouple and the pyrometer during heating was $\sim 3.1\%$ and $\sim 1.9\%$ during the cooling process. Thus it was concluded that the process reached thermal equilibrium, and, since both temperatures agree during equilibrium, the data from the pyrometer was said to be real.

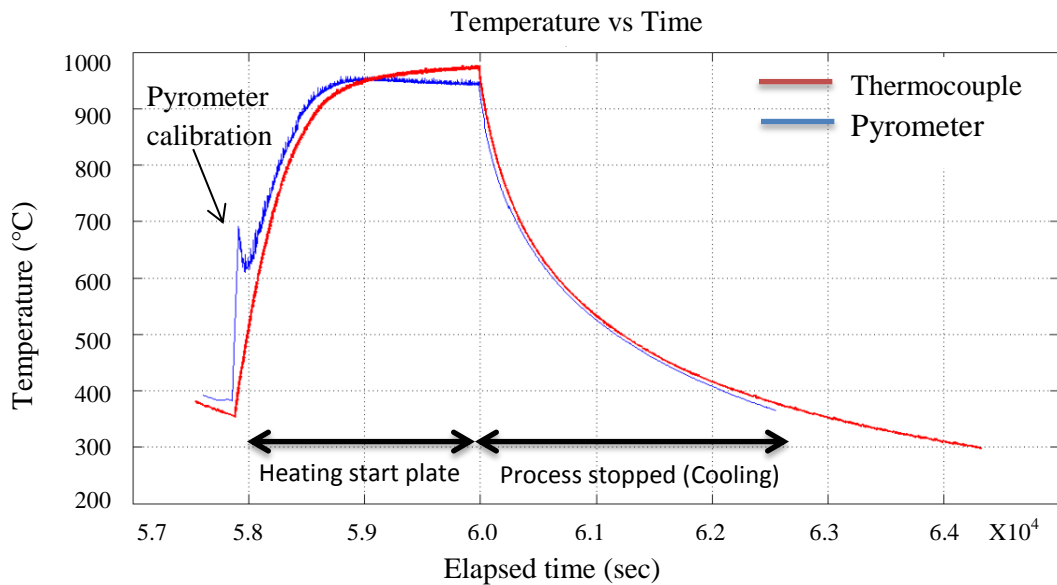


Figure 7. Experiment for comparison of surface temperature between the multi-wavelength pyrometer and the system's thermocouple.

3.1 Characterization of the EBM process

The surface temperature during the fabrication process is important when developing parameters for novel materials, because it allows the user to 1) determine if the appropriate temperature was reached to obtain proper sintering of the material, 2) determine if the melting point of the material was reached during the melting cycle, 3) if a high enough temperature was reached before melting to prevent high voltage arcing of the electron beam, and 4) observe temperature effects due to powder deposition (e.g.,

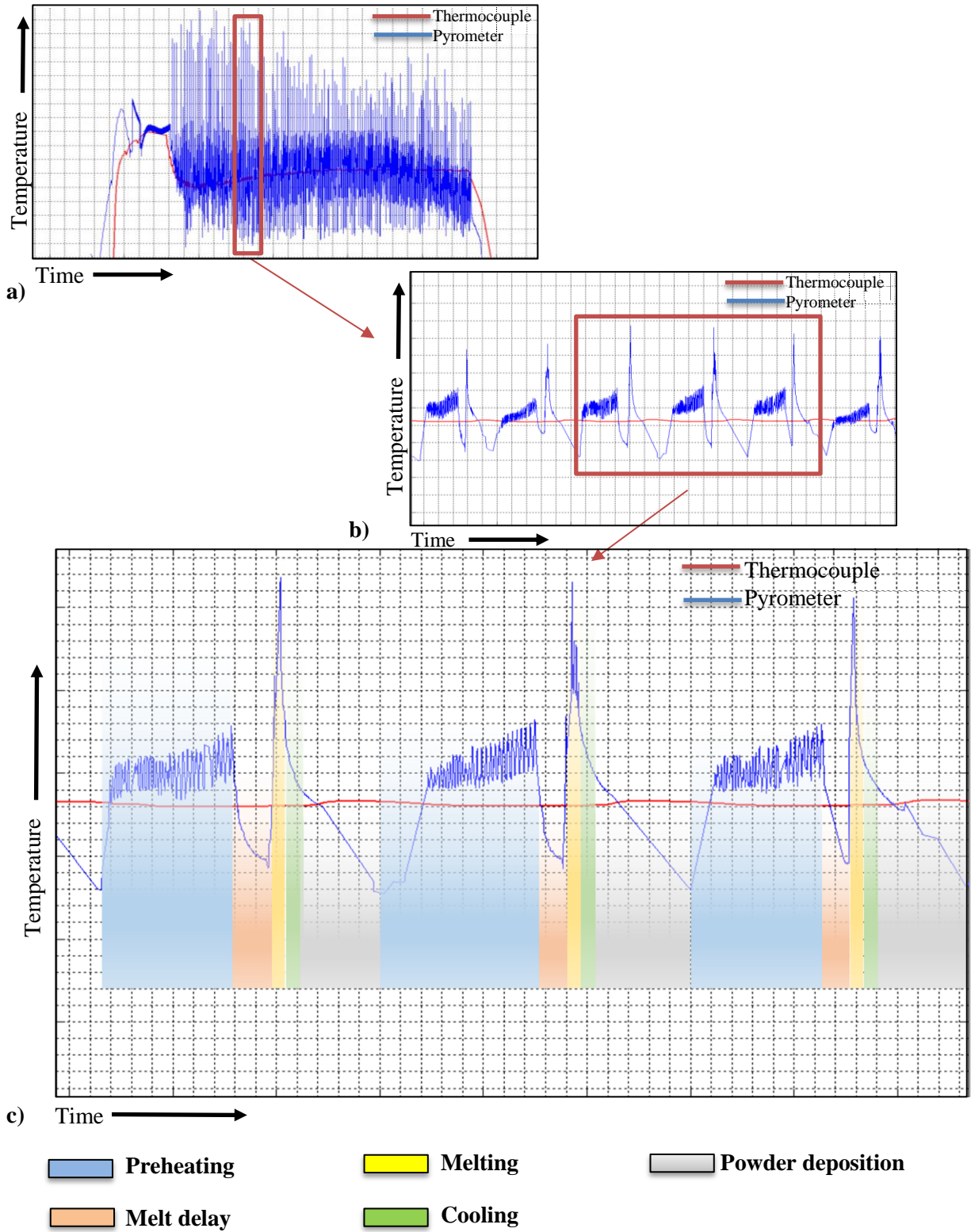


Figure 8. Characterization of the EBM process using the multi-wavelength pyrometer; a) temperature graph; b) surface temperature pattern; c) characterization of the EBM process

excess cooling upon powder deposition). Furthermore, the operator can ensure that a desired surface temperature was obtained after each step to help improve process isotropy. Figure 8a shows a MATLAB graph with the multi-wavelength pyrometer plot (blue) and the thermocouple plot (red) from the experiment described in Figure 5c. The temperature plot from the multi-wavelength pyrometer oscillates throughout fabrication, which can be due to the recording of data during various stages of fabrication which yield different reflections (e.g., powder, melted surface, rake mechanism during powder deposition, etc.). Also, the peaks that describe the melting temperature of the material are not the same every layer. This can be caused by the time delay of the pyrometer recording the temperature data (i.e., melting occurs faster than data logging) or inherent layer-to-layer variations (e.g., different packing of powder that yield variations in melting process and emissivity). Figure 8b is a zoomed view from the graph in Figure 8a, which describes the surface temperature pattern of three consecutive layers during the fabrication process. Figure 8d is the characterization of the EBM process during this experiment. The process consisted of preheating, part melt delay, melting, cooling, and powder deposition.

4. Conclusions

For this project, a multi-wavelength pyrometer was installed in an EBM system and the following was achieved:

1. The multi-wavelength pyrometer was installed in an EBM system. A setup procedure was implemented using quartz glass that helped maintain appropriate transmittance of electromagnetic radiation. A radiation shield was designed and fabricated to prevent radiation exposure and ensure the instrument was safely installed.
2. The multi-wavelength pyrometer data was compared to thermocouple temperature data to determine if the pyrometer measurements were reasonable.
3. The multi-wavelength pyrometer permitted the characterization of the EBM process by identifying the pre-heat temperature, melting temperature, cooling after melting, and powder deposition steps which allow a better understanding of the thermal behavior during fabrication.

An advantage of using the multi-wavelength pyrometer was the capability to obtain real surface temperature measurements without the need to know and define emissivity. The data obtained can be ultimately used as feedback in a closed-loop control system allowing full spatial and temporal control of microstructure through direct modification of melting. Such control can lead to components with improved thermal isotropy and help identify resulting microstructure/mechanical properties of fabricated parts. Furthermore, this information can help facilitate process parameter development for novel materials using EBM or other AM technologies through the improved system feedback.

Acknowledgements

The research described in this paper was performed at the W.M. Keck Center for 3D Innovation at the University of Texas at El Paso (UTEP). Students at the Center, Philip A. Morton and Cesar A. Terrazas, helped perform, and provided advice on, experiments pertaining to the presented research. The authors are also thankful for additional funding of this research that was provided by GE Global Research.

References

Cormier, Denis, Ola Harrysson, and Harvey West. "Characterization of H13 steel produced via electron beam melting." *Rapid Prototyping Journal* 10.1 (2004): 35-41.

Dinwiddie, Ralph B., et al. "Thermographic in-situ process monitoring of the electron-beam melting technology used in additive manufacturing." *SPIE Defense, Security, and Sensing*. International Society for Optics and Photonics, 2013.

Felice, Ralph A. "The spectropyrometer-a practical multi-wavelength pyrometer." *Temperature: Its Measurement and Control in Science and Industry; Volume 7, Part 2* 684 (2003): 711-716.

Felice, Ralph A. "Investment Casting Temperature Measurement." *Foundry Management and Technology* 134.8 (2006): 40-41.

Felice, Ralph A. "Expert System Spectropyrometer Results for Non-Black, Non-Grey, or Changing Emissivity and Selectively Absorbing Environments." *Electro-Techno-Exposition, Moscow*. 2003.

Gibson, Ian, David W. Rosen, and Brent Stucker. *Additive manufacturing technologies*. New York: Springer, 2010.

Mireles, Jorge. "Process Study and Control of Electron Beam Melting Technology Using Infrared Thermography". El Paso: PLC, 2013. Thesis

Price, Steven, *et al.* "Experimental Temperature Analysis of Powder-based Electron Beam Additive Manufacturing". *Solid Freeform Symposium* (2013): 162-173

Rodriguez, Emmanuel. "Development of a Thermal Imaging Feedback Control System in Electron Beam Melting". El Paso: ProQuest LLC, 2013. Thesis.

Sclater, Neil and Nicholas P. Chironis. *Mechanisms and Mechanical Devices Sourcebook*. New York: McGraw-Hill Professional, 2006.